XVI International Conference on Durability of Building Materials and Components
DBMC 2023, China
K.F. Li and D.P. Fang (Eds)

Impact of the Thaumasite Sulfate Attack on the Pore Structure and Gas Permeability of Cement Mortar

Bo Ran[1], Tingyu Hao[2], Xiaobin Hao[2] and Kefei Li[1]

[1] Department of Civil Engineering, Tsinghua University, Beijing 100084, PR China, rb17@mails.tsinghua.edu.cn (Bo Ran), likefei@tsinghua.edu.cn (Kefei Li)

[2]Central Research Institute of Building and Construction, China Metallurgical Group Corporation, Beijing, 10088, China, haotingyu@cribc.com (Tingyu Hao), hao_xiaobin123@163.com (Xiaobin Hao)

Abstract. *In this study, the impact of the thaumasite sulfate attack (TSA) on cement mortar was investigated by comparing it to the ettringite sulfate attack (ESA). Mortar specimens with three binders, corresponding to the blank, ESA, and TSA, were exposed to sulfate solution. The evolutions of thaumasite and ettringite formation, pore structure, and gas permeability on the mortar specimens were characterized through XRD, ^{1}H NMR, and CemBureau device. The experimental results show that: (1) both ettringite and thaumasite were formed in TSA; (2) ESA reduces the capillary pore space, whereas TSA decreases both the capillary pore and interlayer pores; and (3) ESA decreases the gas permeability while TSA significantly increases it.*

Keywords: *Cement mortar, Sulfate attack, Thaumasite, Ettringite, Gas permeability.*

1 Introduction

External sulfate attack is a major concern for the durability of cement-based materials (CBM) subjected to sulfate-bearing environments, and thaumasite and ettringite are two main products during the attack process, corresponding to two sulfate attack forms: ettringite sulfate attack (ESA) and thaumasite sulfate attack (TSA). Ettringite results from the reaction between the aluminium phase in cement paste and sulfates, and it leads to the expansion and spalling damage of CBM (Marchand et al. 2002). Thaumasite is the product of the low-temperature reaction between calcium silicate hydrates (CSH) and sulfates and carbonates, resulting in the consumption of CSH and the ensuing loss of adhesion and strength (Crammond 2002). The mechanism of ESA has been deeply understood through extensive research, and there are sufficient preventative measures in engineering practise. However, a systematic study of TSA is still lacking.

TSA has been well investigated in recent years, but the focus has been on the chemical reaction mechanism. Schmidt and Lothenbach (2008) determined the dissolution constant of thaumasite through a progressive equilibrium approach and found the essential role of calcite in the thaumasite formation. Köhler and Heinz (2006) proposed that the thaumasite is formed through heterogeneous nucleation on the ettringite surface. Bellmann and Stark (2008) reported that the addition of calcium hydroxide increased the calcium/silicon ratio of CSH and favoured thaumasite formation. These studies reveal the formation mechanism of thaumasite and its influential factors, but there is little research studying the impact of TSA on the durability properties of CBM, especially the pore structure and transport properties. To this objective, this

study designs three mortar mix ratios corresponding to blank, ESA, and TSA and examines the changes in pore structure and gas permeability of the three mortar mixtures with time.

2 Experimental Program

2.1 Specimen Preparation

Three cement mortar mixtures were prepared using Ordinary Portland Cement (OPC), limestone with a $CaCO_3$ content exceeding >98 wt%, and gypsum with a $CaSO_4$ content exceeding 99 wt%. The chemical composition of OPC and the mix proportions of cement mortars are given in Table 1 and Table 2, respectively. The cement mortars were cast as cylinders with a diameter of 100 mm and a height of 200 mm, and then cured in a moist room at 20 ^oC and 95% relative humidity for 28 days. From the cylinders, large disks of Φ100 mm×50 mm were produced for gas permeability tests, while small cylinders of Φ25 mm×25 mm were produced for ^1H NMR analysis. All the specimens were immersed into a sulfate solution of 1.63 g/L SO_4^{2-} in Na_2SO_4 within a refrigerating cabinet at a temperature of 10 ^oC, and the test solution was replaced on biweekly basis. At given exposure ages, the disks were removed and dried at 60 ^oC prior to the permeability test, and after the test some powders were ground from the cylinders for XRD analysis. The small cylinders were subjected to the ^1H NMR test directly and then re-immersed into the sulfate solution due to the non-destructive character of the ^1H NMR method.

Table 1. Chemical composition of OPC.

Components %							
CaO	SiO	Al_2O_3	Fe_2O_3	MgO	SO_3	K_2O	Na_2O
58.75	21.39	7.44	3.23	3.39	2.02	0.84	0.35

Table 2.Mix proportions of cement mortars (kg/m^3).

	Cement	Gypsum	Limestone	Water	Sand
MC	490	0	122	306	1320
MG	551	61	0	306	1320
MI	428	61	122	306	1320

2.2 Experimental Methods

The experiments in this study include XRD for the identification of mineral phases, ^1H NMR for microstructure characterization, and gas permeability measurements for transport property analysis.

2.2.1 X-ray diffraction

The device for identifying the mineral phases was a D8 Advance X-ray diffractometer (Bruker) and the XRD tests were performed on powder samples using Cu radiation at an angular step of 0.02^o per second between 5^o and 75^o [2θ].

2.2.2 ^1H NMR

The device for the 1H NMR test was a VTMR20-010V-I spectrometer (Niumag) at 0.5 T with field stability and a drift rate <200 Hz/h. A 90° pulse length of 2.8 μs was set, and a typical Carr-Purcell-Meiboom-Gill (CPMG) measurement with a repetition delay of 1 s was adopted.

2.2.3 Gas permeability

The gas permeability test follows the CemBureau method (Kollek 1989), which specifies a 1D gas flow under a constant pressure gradient. The device used in this study has been previously described in publications (Gui et al. 2016, Zhang and Li 2019) and the infiltrating gas is nitrogen. The gas permeabilities were evaluated through Darcy's law under diffierent gas pressure gradients, and the intrinsic permeability was determined from the relation between gas permeabilities and pressure gradients, i.e., the Klinkenberg's corretion (Klinkenberg 1941),

$$k_A = k_0(1 + b/P_m) \tag{1}$$

Where, k_A stands for gas permeability, k_0 for intrinsic permeability, b for the Klinkenberg factor, and P_m the average pressure of two pressures for the gradient.

3 Results and Analysis

3.1 Mineral Phases

Figure 1 presents the XRD results of three mortar specimens at different immersion ages. According to Figure 1a, the phase peaks of ettringite and thaumasite do not increase (even slightly decrease) with immersion time, indicating that neither ettringite nor thaumasite were formed in MC specimens during the immersion. Figure 1b shows that the ettringite peak increases with the immersion time, while the thaumasite almost remains unchanged, indicating that only ettringite was formed during the immersion. In Figure 1c, the ettringite peak obviously rises in the first 4 months and then decreases, accompanied by an increase in the thaumasite peak in the 8-month age, indicating that both ettringite and thaumasite were produced during immersion in the MI specimens. The XRD results suggest that: (1) ettringite is formed prior to

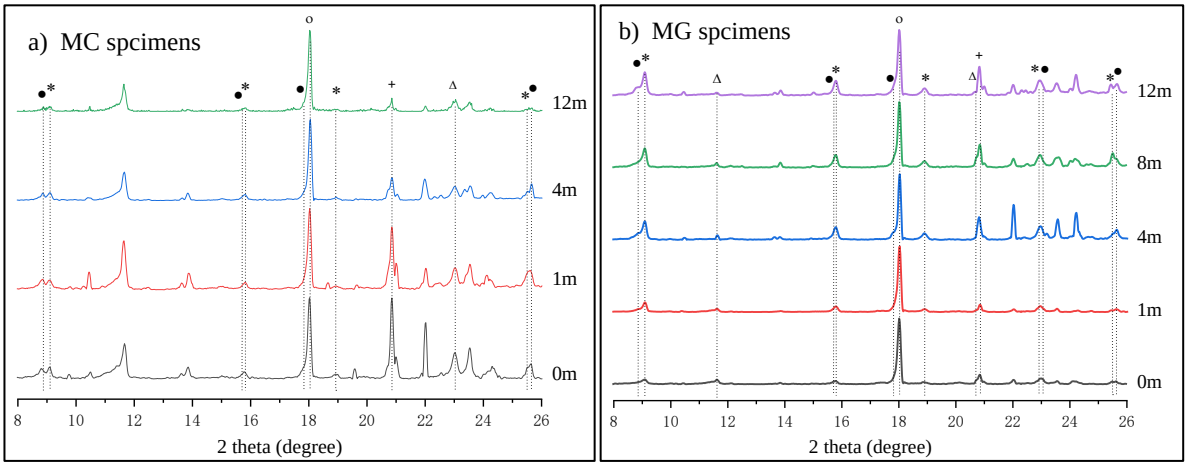

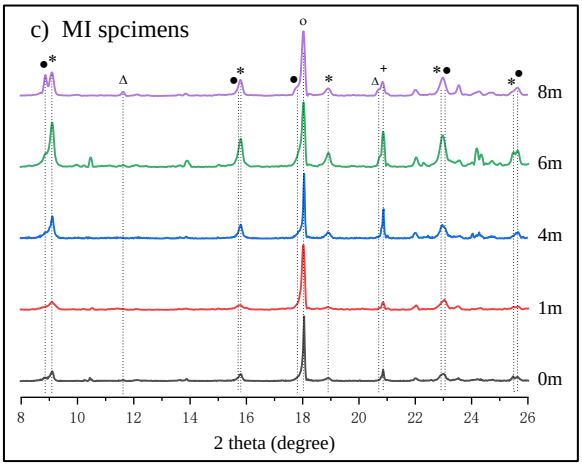

Figure 1. XRD profiles of MC (a), MG (b) and MI (c) specimens after immersion into sulfate solution for different ages. The solid circle (●), asterisk (*), hollow circle (○), and the plus sign (+) denote thaumasite, ettringite, protlandite and quartz. The triangle (Δ) represents calcite in MC specimens and gupsum in MG and MI specimens.

thaumasite, which is consistent with Schmidt et al.'s finding (2008); (2) the formation of thaumasite requires high concentrations of sulfate and carbonate.

3.2 ^{1}H NMR

Figure 2 presents the transverse relaxation time (T2) distributions of three mortar specimens at different immersion ages. Based on She et al.'s study (2010), the T2 values in the range of 0.01-1 ms correspond to the interlayer and gel water (with interlayer water having a smaller T2 value than gel water), and 1-100 ms correspond to the capillary water. In Figure 2a, a slight reduction in capillary pores was observed, which is indicative of continuous hydration. The capillary pores volume drops and the gel pores volume rises with the immersion time in Figure 2b, suggesting that the ettringite precipitated in capillary pores, which is in line with the findings in the previous work (Ran et al., 2023). Figure 2c shows a decreasing trend in capillary pore space and an increasing trend in gel pore space, with the int erlayer pore decreasing after 8-

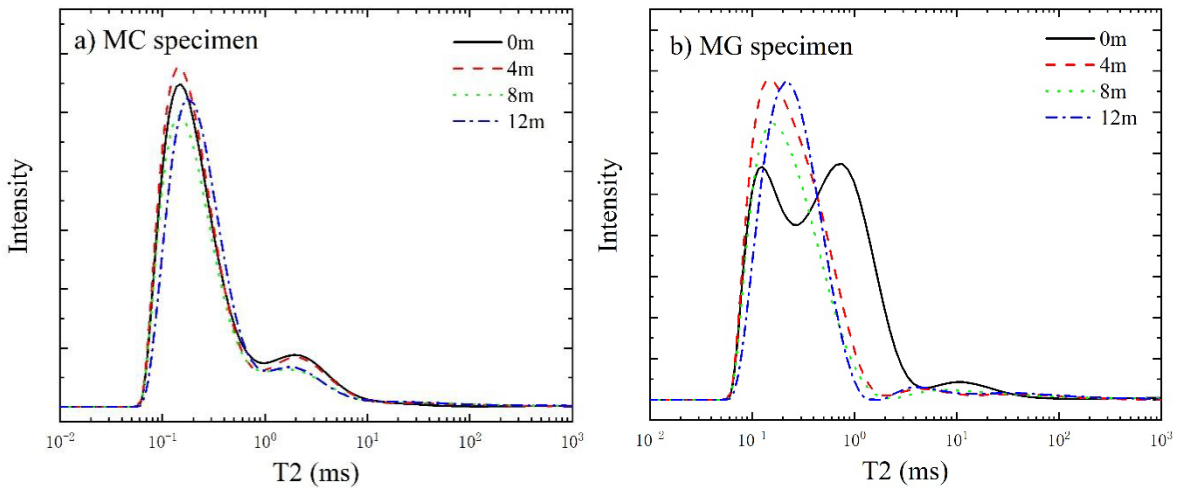

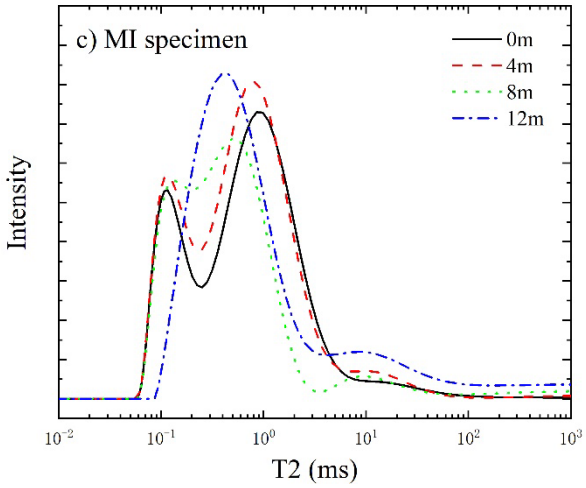

Figure 2. T2 distributions of MC, MG and MI specimens after immersion into sulfate solution for different ages.

month immersion for MI specimens. Combined with the XRD results in Figure 1c, a damage process for TSA is proposed as follows: initially, ettringite was formed and filled the capillary pore; afterwards, the formation of thaumasite consumed CSH gel, leading to the decrease of the interlayer pore (around 0.1 ms). Besides, the formation of non-gelling powdery thaumasite correlates to the increase in large capillary pores (10-20 ms).

3.3 Gas Permeability

Figure 3 presents the change in gas permeabilities for three mortar specimens with immersion time. According to Figure 3a, the initial intrinsic permeability of the MI specimen is approximately four times higher than that of the MC and MG specimens, indicating better pore connectivity in the MI specimen after curing. Additionally, the intrinsic permeability of the MC and MG specimens decreases with immersion time, which can be attributed to the ongoing

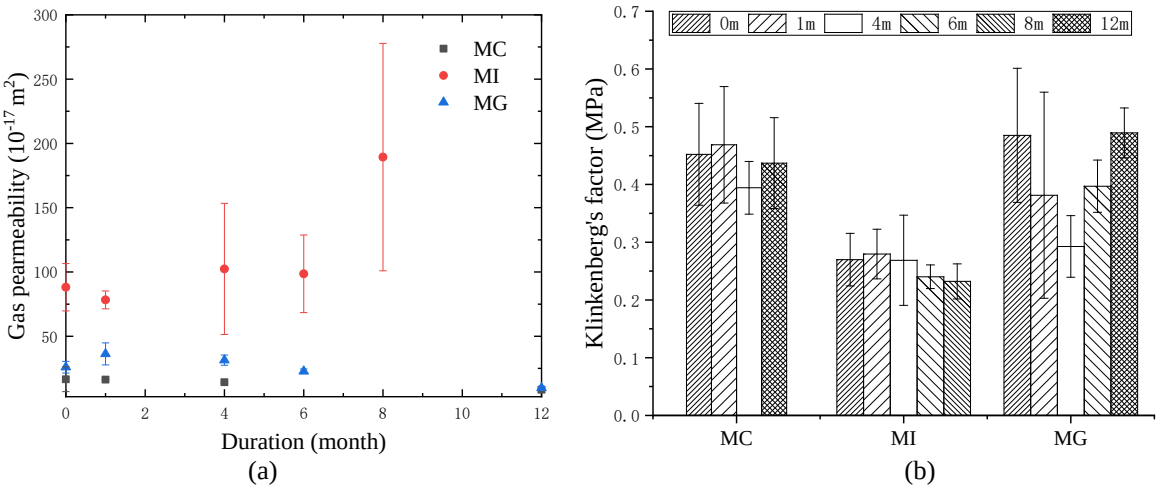

Figure 3. Intrinsic permeabilities (a) and Klinkenberg factors (b) of MC, MG and MI specimens after immersion into sulfate solution for different ages.

hydration of cement paste and the precipitation of ettringite. However, the intrinsic permeability of the MI specimen shows an increasing trend during the immersion process and substantially rises at 8-month age, which corresponds to the formation of thaumasite in Figure 1c and the decrease of interlayer pore space in Figure 2b. The increase in the intrinsic permeability of cement mortar by the formation of thaumasite is attributable to the consumption of the CSH gel, which leads to the transformation of interlayer pores into large capillary pores in Figure 2b, improves the pore connectivity, and thus increases the intrinsic permeability. In Figure 3b, the Klinkenberg factor of MI specimens is only about half that of the MC and MG specimens, which reveals a better pore connectivity of MI specimens than MG and MC specimens (Zhang and Li 2019).

4 Conclusions

- Ettringite forms in high sulfate condition, while thaumasite only forms in high sulfate-carbonate environments. In TSA, ettringite is formed prior to thaumasite, and the formation of thaumasite consumes part of ettringite.
- Ettringite precipitates in capillary pores, and the formation reaction of thaumasite converts the interlayer pore into large capillary, corresponding to the decrease in intensity of the T2 value around 0.1ms and the increase in T2 value ranging between 10 and 20ms.
- ESA reduces the intrinsic permeability of cement mortar, while TSA improves the pore connectivity, resulting in an increase in the intrinsic permeability and a decrease in the Klinkenberg factor.

Acknowledgements

The research is supported by the open Project Fund (No.JZA2018Kj03) of. China Metallurgical Group Corporation.

References

Bellmann, F., and Stark, J. (2008). *The role of calcium hydroxide in the formation of thaumasite*. Cement and Concrete Research, 38(10), 1154-1161.

Crammond, N. (2002). *The occurrence of thaumasite in modern construction–a review*. Cement and Concrete Composites, 24(3-4), 393-402.

Gui, Q., Qin, M., and Li, K. (2016). *Gas permeability and electrical conductivity of structural concretes: Impact of pore structure and pore saturation*. Cement and Concrete Research, 89, 109-119.

Klinkenberg, L. J. (1941). *The permeability porous media to liquids gases*. American Petroleum Institute Drilling and Production-Practice.

Köhler, S., Heinz, D., and Urbonas, L. (2006). *Effect of ettringite on thaumasite formation*. Cement and Concrete Research, 36(4), 697-706.

Kollek, J. J. (1989). *The determination of the permeability of concrete to oxygen by the Cembureau method—a recommendation*. Materials and structures, 22, 225-230.

Marchand, J., Odler, I., and Skalny, J.P. (2001). *Sulfate attack on concrete*. CRC Press.

Ran, B., Omikrine-Metalssi, O., Fen-Chong, T., Dangla, P., and Li, K. (2023). *Pore crystallization and expansion of cement pastes in sulfate solutions with and without chlorides*. Cement and Concrete Research, 166, 107099.

Schmidt, T., Lothenbach, B., Romer, M., Scrivener, K., Rentsch, D., and Figi, R. (2008). *A thermodynamic and experimental study of the conditions of thaumasite formation*. Cement and Concrete Research, 38(3), 337-349.

She, A. M., and Yao, W. (2010). *Research on hydration of cement at early age by proton NMR*. J. Build. Mater, 13(703), 377-380.

Zhang, D., and Li, K. (2019). *Concrete gas permeability from different methods: Correlation analysis*. Cement and Concrete Composites, 104, 103379.